Thermodynamics of Shear-Induced Phase Transitions for Multicomponent Fluid Mixtures

Wilson A. Cañas-Marín
Instituto Colombiano del Petróleo, ECOPETROL-ICP S.A., Piedecuesta-Santander, Colombia

DOI 10.1002/aic.14160
Published online June 21, 2013 in Wiley Online Library (wileyonlinelibrary.com)

A thermodynamic approach for modeling the phase equilibrium of multicomponent fluid mixtures under the influence of an applied shear rate (shear stress) is presented. This approach is based on assuming that, for the modeled mixtures, the viscosity variation with shear rate can be well-described by using a power law. This framework is then used for predicting the influence of shear rate on the critical temperature, critical pressure, and spinodal curve of several Newtonian multicomponent hydrocarbon mixtures; giving as a result that for these kind of mixtures and depending on the composition, the critical temperature exhibits both an upward and downward shift with shear rate, whereas the critical pressure always exhibits a downward trend. Both a suppression of the liquid–liquid transition and shrinkage of the spinodal curves (mixing effect) are also predicted. © 2013 American Institute of Chemical Engineers *AIChE J*, 59: 4383–4389, 2013

Keywords: thermodynamics, shear-induced, critical point, spinodal curve, viscosity

Introduction

Fundamental models have been developed for describing the effects of external force fields on the phase properties of physicochemical systems.[1–3] Nonetheless, there seem to be discrepancies among the different formulations proposed particularly due to the definition of the work done by the external field and the mathematical approach used for expressing the effect of the particular field in terms of a proper combination of extensive and intensive variables.[4]

It is well-known that flow can strongly influence the degree of mixing in polymer solutions, and, a lesser degree, polymer blends. Silberberg and Kuhn[5] were the first in experimentally observing phase transitions influenced by flow. Shear-induced effects on the critical temperature and spinodal curve of polymers and blends under flow conditions have been widely studied experimentally; observations are usually based on the appearance of turbidity in the solution under flow, as compared with the solution at rest. Other techniques for studying this phenomenon are based on the analysis of light scattering signals or by changes in viscosity.[6,7] Both shear-induced mixing and demixing of polymer blends have been reported.[6,7] For example, Hindawi et al.[8] reported that both a shear-induced demixing and mixing effect may be observed within the same blend depending on the magnitude of the applied shear and also that the magnitude of the increase or decrease in the lower critical solution temperature varies depending upon the blend composition. Chopra and Vlassopoulos[9] found experimentally that, depending on temperature, both shear-induced mixing, usually at very high shear rates, and shear-induced demixing, typically at moderate shear rates, could be observed in poly (styrene-co-maleic anhydride)/poly(methyl methacrylate) blends. Moreover, nearly two decades ago, Rangel-Nafaile et al.[10] measured shifts up to 20°C or more in cloud points of high-molecular-weight polystyrene solutions in dioctylphtalate as a function of flow rate, that is, for increasing values of applied shear stress, the turbidity curves are shifted to higher temperatures. For low-molecular-weight solutions, the effect seems to be strongly reduced and is supposed to suppress concentration fluctuations (shear-induced mixing).[11] For instance, Hanley and Evans found that the transition of a Lennard–Jones fluid from gas to liquid is suppressed by a shear (i.e., mixing effect).[12]

The influence of shear flow has also been theoretically studied: for instance, Ver Strate and Philippoff[13] introduced a quasi-chemical approximation based on the assumption that the enhanced or reduced scattering observed corresponds to a real and genuine-phase transition. This approach was then advanced mainly by Rangel-Nafaile et al.[10] and Wolf.[14] In short, the approach is based on a Flory–Huggins-type description that includes the influence of flow by introducing a concentration-dependent stored free-energy term developed originally by Marrucci.[15] This approach has been criticized by several researchers because it has no clear basis in statistical mechanics.[16,17] Rangel-Nafaile et al.[10] followed the classical thermodynamics in contrast to the recent theories on polymer solutions. Casas-Vásquez et al.,[18] nonetheless, stressed that thermodynamic arguments, in view of the still weak predicting power of the dynamical theory, could be useful in understanding shear effects in polymers; for example, whether the flow-induced miscibility experimental

Additional Supporting Information may be found in the online version of this article.

Correspondence concerning this article should be addressed to Wilson A. Cañas-Marín at wilson.cmarin@ecopetrol.com.co

results in polymer mixtures really result from a true change of the spinodal curve or whether they are a hydrodynamic effect.

Roming and Hanley[19] developed a thermodynamic approach based on nonequilibrium molecular dynamics studies for a model Lennard–Jones liquid, and then they applied their approach for modeling Lennard–Jones binary mixtures via a modified conformal solution one-fluid approach. The main findings were that a sufficient shear could significantly affect the fluid-phase behavior of this kind of model mixture, suppressing the liquid–liquid-phase separation and enlarging the mixture's homogeneous region (i.e., mixing effect).

Polymers are not the only real systems where an applied shear could produce changes upon its phase behavior. In principle, all systems under flow are influenced to some extent by an applied shear rate (stress). For instance, the petroleum and food industries are two examples where knowing the shear-induced effects could be very important.[20,21] In petroleum reservoir production, complex and multicomponent mixtures (gases, oils, and water) must travel away from the reservoir up to surface and are subjected to changes in shear stresses. Therefore, it is important to be able to model the actual effect of applied shear on the thermodynamic-phase behavior of these fluids and to evaluate whether the applied shear induces the mixing or demixing of the mixture transported or promotes the precipitation of very undesirable phases such as paraffinic solids or asphaltenes, which jeopardize the production.[20] In the food industry, many products are crystallized under shear because mixing enhances the heat-transfer rate and helps to produce homogeneous crystals.[21]

Occasionally, models based on classical irreversible thermodynamics, extended irreversible thermodynamics (EIT),[22] or machine calculations[23] are not practical or easily usable in complex and real multicomponent mixtures. For example, it is presently unclear how to evaluate terms such as the "steady-state compliance" in the EIT framework for complex and multicomponent mixtures such as those found in the petroleum industry (Jou D. *Personal Communication*, 2003). Due to these drawbacks, the objective of this work is twofold: first, derive and present a novel, robust and consistent thermodynamic framework for explicitly modeling the shear effect on the thermodynamics of pure components and multicomponent mixtures. Second, apply the thermodynamic framework derived for predicting whether a shear rate really "shifts" the critical temperature, the critical pressure, and spinodal curve of five real fluid mixtures and compares the magnitudes and trends of these shifts against theoretical predictions and experimental measurements; these last ones based on small angle light scattering (SALS) and turbidity measurements published in the literature.

Thermodynamics of Shear-Induced Phase Transitions

If a homogeneous and closed system of variable volume is subjected to a reversible process of compression or expansion against an external pressure,P, then the work done over the system is given by[2]

$$dW = -PdV \tag{1}$$

Following Haase,[24] if additionally a shear stress is applied on the above system then the total work done over such a system may be expressed as

$$dW = -PdV + \tau d(\dot{\gamma}V) \tag{2}$$

Here τ and $\dot{\gamma}$ are shear stress and shear rate, respectively.

In Eq. 2, both contributions are the product between an intensive property (P,τ) and a differential extensive property $(dV + d(\dot{\gamma}V))$. Therefore, Eq. 2 may be compacted as

$$dW = \sum_i L_i dl_i \tag{3}$$

Subscript i extends to every type of work depending on the internal coordinates of the system or interest region. l_i and L_i are called work coordinates (extensive quantity) and conjugated work coefficients (intensive quantity), respectively. When the temperature and composition of the system are known, the internal state of the system is given empirically by variables l_i and L_i. Forces depending on the variation of the external coordinates of the system (e.g., gravitational, centrifugal, and acceleration) or on the presence of irreversible processes (e.g., friction forces) should not be interpreted as work coefficients, L_i.[24]

From the first law of thermodynamics for a reversible change in a closed-system internal state

$$dU = TdS + \sum_i L_i dl_i \text{ or } TdS = dU - \sum_i L_i dl_i \tag{4}$$

Equation 4 expresses that the entropy (S) depends on internal energy (U) and on the work coordinates at (l_i), keeping constant the quantities of each substance (n_j). Differentiating Eq. 4

$$T\left(\frac{\partial S}{\partial U}\right)_{l_i,\mathrm{n_j}} = 1, T\left(\frac{\partial S}{\partial l_i}\right)_{U,l_{j\neq i},n_j} = -L_i \tag{5}$$

As entropy also depends on the quantity of substance, analogously with work coefficients and coordinates, chemical potential can be defined as

$$\mu_i \equiv -T\left(\frac{\partial S}{\partial n_i}\right)_{U,l_j,n_j\neq k} \tag{6}$$

Therefore, from Eqs. 3–6, a generalized form of the Gibbs equation is obtained for the derivative of the entropy into a region of variable quantity and composition (open system)

$$TdS = dU - \sum_i L_i dl_i - \sum_{i=1}^{NC} \mu_i dn_i \tag{7}$$

From Legendre transforms,[25] it is possible to define other extensive thermodynamic potentials such as

$$H \equiv U - \sum_i L_i l_i; A \equiv U - TS; G \equiv A - \sum_i L_i l_i \tag{8}$$

Here H, A, G are enthalpy, Helmholtz, and Gibbs free energies, respectively.

Differentiating the expressions in Eq. 8 and using Eq. 7, the corresponding fundamental equations are obtained as

$$dU = TdS + \sum_i L_i dl_i + \sum_{i=1}^{NC} \mu_i dn_i \tag{9}$$

$$dH \equiv TdS - \sum_i l_i dL_i + \sum_{i=1}^{NC} \mu_i dn_i \tag{10}$$

$$dA \equiv -SdT + \sum_i L_i dl_i + \sum_{i=1}^{NC} \mu_i dn_i \tag{11}$$

$$dG \equiv -SdT - \sum_i l_i dL_i + \sum_{i=1}^{NC} \mu_i dn_i \tag{12}$$

whose characteristic functions are $U(S, l_i, n_j)$, $H(S, L_j, n_j)$, $A(T, l_i, n_j)$, and $G(T, L_j, n_j)$, respectively.

Equation 11 will be used in this work for deducting an expression of chemical potential modified by a shear rate contribution. But similar expressions based on Eq. 12 and as a function of shear stress are available in Appendix.

For a system subjected to a pressure–volume work and in presence of a shear effect, Eq. 11 is reduced to

$$dA = -SdT - PdV + \tau d(V\dot{\gamma}) + \sum_{i=1}^{NC} \mu_i dn_i \tag{13}$$

T, V, n_j, and $\dot{\gamma}$ are then the independent variables of interest. Then, differentiating Eq. 13 and collecting terms

$$dA = -SdT - [P - \tau\dot{\gamma}]dV + (\tau V)d\dot{\gamma} + \sum_{i=1}^{NC} \mu_i dn_i \tag{14}$$

From Eq. 14, the following Maxwell relation can be obtained

$$\left(\frac{\partial(\tau V)}{\partial n_i}\right)_{T,V,\dot{\gamma},n_{j\neq i}} = \left(\frac{\partial \mu_i}{\partial \dot{\gamma}}\right)_{T,V,n_j} \tag{15}$$

Here, we assume that the shear stress and the respective shear rate are related by the following constitutive equation

$$\tau = \eta(\dot{\gamma})\dot{\gamma};\ \text{where}\ \eta(\dot{\gamma}) = \bar{\kappa}\dot{\gamma}^{\xi-1} \tag{16}$$

substituting Eq. 16 in Eq. 15 produces

$$V\dot{\gamma}^{\xi}\left(\frac{\partial \bar{\kappa}}{\partial n_i}\right)_{T,V,\dot{\gamma},n_{j\neq i}} = \left(\frac{\partial \mu_i}{\partial \dot{\gamma}}\right)_{T,V,n_j} \tag{17}$$

By integrating Eq. 17

$$\int_{\mu_i}^{\tilde{\mu}_i} d\mu_i = \int_{\dot{\gamma}=0}^{\dot{\gamma}} \left[V\left(\frac{\partial \bar{\kappa}}{\partial n_i}\right)_{T,V,\dot{\gamma},n_{j\neq i}}\right]\dot{\gamma}^{\xi} d\dot{\gamma} \tag{18}$$

Then

$$\tilde{\mu}_i(\dot{\gamma}) = \mu_i(\dot{\gamma}=0) + \frac{v}{(\xi+1)}\left[n_T\left(\frac{\partial \bar{\kappa}}{\partial n_i}\right)_{T,V,\dot{\gamma},n_{j\neq i}}\right]\dot{\gamma}^{(\xi+1)};\ i = 1...NC \tag{19}$$

where $V = n_T v$ has been used.

Defining $\tilde{\mu}_i$ in terms of fugacity

$$\tilde{\mu}_i(T, V, n_i, \dot{\gamma}) \equiv RT\ln\tilde{f}_i(T, V, n_i, \dot{\gamma}) + \mu_i^0(T) \tag{20}$$

and using the traditional definition

$$\mu_i(T, V, n_i) \equiv RT\ln f_i(T, V, n_i) + \mu_i^0(T) \tag{21}$$

where $\mu_i^0(T)$ is the reference chemical potential for the pure component assumed as an ideal gas at T and $P = 1$ bar (or 1 atm).

Eq. 19 can be then expressed as

$$\tilde{f}_i(\dot{\gamma}) = f_i(\dot{\gamma}=0)\exp\left(\frac{v}{(\xi+1)RT}\left[n_T\left(\frac{\partial \bar{\kappa}}{\partial n_i}\right)_{T,V,\dot{\gamma},n_{j\neq i}}\right]\dot{\gamma}^{(\xi+1)}\right);\ i = 1...NC \tag{22}$$

In Eq. 19 or 22, it is necessary to evaluate $\left(\frac{\partial \bar{\kappa}}{\partial n_i}\right)_{T,V,\dot{\gamma},n_{j\neq i}}$ to be able to evaluate the $\dot{\gamma}$ effect on the phase behavior of a multicomponent fluid mixture. For a Newtonian mixture, $\xi = 1$; and then from Eq. 16, $\bar{\kappa} = \eta$(i.e., viscosity is independent of shear rate). In this last case, Eqs. 19 and 22 are, respectively, simplified to

$$\tilde{\mu}_i(\dot{\gamma}) = \mu_i(\dot{\gamma}=0) + \frac{v}{2}\left[n_T\left(\frac{\partial \eta}{\partial n_i}\right)_{T,V,\dot{\gamma},n_{j\neq i}}\right]\dot{\gamma}^2 \tag{23}$$

$$\tilde{f}_i(\dot{\gamma}) = f_i(\dot{\gamma}=0)\exp\left(\frac{v}{2RT}\left[n_T\left(\frac{\partial \eta}{\partial n_i}\right)_{T,V,\dot{\gamma},n_{j\neq i}}\right]\dot{\gamma}^2\right) \tag{24}$$

Note that, from Eq. 19 or 22 (or Eq. 23 or 24 for Newtonian fluids), the shear has no a direct effect on the chemical potential (or fugacity) of a pure fluid if T, V, n_j, and $\dot{\gamma}$ are taken as the independent variables.

As the pressure here is a dependent variable, then the shear rate should have an effect on it. From Eq. 14 and taking T, V, n_j as constants,

$$dA = \tau V d\dot{\gamma} \tag{25}$$

By integration of Eq. 25

$$\int_{A_0}^{A} dA = \int_{\dot{\gamma}=0\dot{\gamma}} V\bar{\kappa}\dot{\gamma}^{\xi} d\dot{\gamma} \tag{26}$$

$$A = A_0 + \left(\frac{V\bar{\kappa}}{\xi+1}\right)\dot{\gamma}^{\xi+1} \tag{27}$$

and taking derivatives with respect to V

$$\left(\frac{\partial A}{\partial V}\right)_{T,n,\dot{\gamma}} = \left(\frac{\partial A_0}{\partial V}\right)_{T,n,\dot{\gamma}=0} + \left(\frac{\bar{\kappa}}{\xi+1}\right)\dot{\gamma}^{\xi+1} \tag{28}$$

giving

$$-P(\gamma) = -P(\gamma=0) + \left(\frac{\bar{\kappa}}{\xi+1}\right)\dot{\gamma}^{\xi+1}, \quad \text{or}$$

$$P(\gamma) = P(\gamma=0) - \left(\frac{\bar{\kappa}}{\xi+1}\right)\dot{\gamma}^{\xi+1} \tag{29}$$

again for a Newtonian mixture

$$P(\gamma) = P(\gamma=0) - \frac{1}{2}\eta\dot{\gamma}^2 \tag{30}$$

and, obviously, for a pure fluid $P(\gamma) \neq P(\gamma=0)$.

To the best of our knowledge, no previous derivation of these equations had been reported in the literature. The thermodynamic framework above (Eq. 19 or 22) can be applied for modeling the effect of a shear rate on the phase behavior of fluid mixtures, provided both T, V, n_j, and $\dot{\gamma}$ are the variables of interest. This thermodynamic framework has a wide range of application for modeling the thermodynamics and phase behavior of mixtures and pure components in petroleum and chemical industry, including solid, liquid, and gas phases, whose changes of viscosity can be described by a power law. Newtonian fluids are only a particular case as it was emphasized before. The application and results obtained with the present model will only depend on the exactitude of the thermodynamic model used to describe the thermodynamics and phase behavior of pure components or mixtures without the shear-rate effect (i.e., $\mu_i(\dot{\gamma}=0)$ or $f_i(\dot{\gamma}=0)$, Eqs. 19 and 22, respectively) and also on a good fitting of viscosity data to the power law represented by Eq. 16. Then, if both conditions above are strictly accomplished, the shear-rate effect (i.e., flow effect) on the thermodynamics and

Table 1. Composition (% mol) of the Five Real Petroleum Reservoir Fluids (F1–F5) Modeled in this Work

	Reservoir Fluids				
	F1 (gas)	F2 (gas)	F3 (oil)	F4 (oil)	F5 (oil)
Component	Composition (mol%)				
CO_2	2.08	4.29	3.95	3.83	3.71
C1N2	**69.65**	**64.18**	**50.77**	**45.03**	**38.05**
C2	8.04	8.93	8.08	7.43	6.49
C3–C4	6.77	7.03	7.05	6.69	6.01
C5–C6	3.06	2.86	3.33	3.32	3.13
C7–C10	5.21	5.48	8.87	9.80	10.31
C11–C14	2.29	2.99	5.16	6.06	7.20
C15–C20	1.81	2.57	4.90	5.32	5.11
C21–C29	0.92	1.25	4.18	5.46	6.39
C30+	0.18	0.43	3.70	7.07	13.59

phase behavior of a given system can be consistently modeled. For instance, for modeling the shear-rate effect on the wax precipitation, an inviolable prerequisite is to have a thermodynamic model able to describe the cloud point threshold and the amount of wax precipitated under these conditions. Obviously, a right viscosity model to represent the non Newtonian behavior exhibited by these waxy mixtures at temperatures lower than the respective cloud point is also required. Progress in this kind of modeling is forthcoming.

Results and Discussion

The thermodynamic framework above derived is here used for predicting whether a shear rate really "shifts" the critical temperature, the critical pressure, and spinodal curve of real multicomponent fluid mixtures. Comparisons of the magnitudes and trends predicted by the present model against theoretical predictions and experimental data based on SALS and turbidity measurements published in the literature are then carried out. For this goal, five real petroleum reservoir mixtures (F1–F5) from South America are used and whose respective compositions are depicted in Table 1, where, based on chromatographic analysis up to C30+, some components were grouped to reduce the computational work. In Table 1, the molar compositions of the "component" C1N2 (combination of methane and nitrogen) are highlighted in bold to emphasize that the fluids F1–F5 cover a wide range of real petroleum reservoir fluid, explicitly from light gases to black oils. Viscosity measurements demonstrated that these five mixtures exhibit Newtonian behavior and the measured viscosity data were fitted using the Lorentz–Bray–Clark (LBC) model, which is very well-known and widely used.[26] Liquid–vapor pressure–volume–temperature data were fitted with the Peng–Robinson equation of state (EoS)[27] to describe the thermodynamics and phase behavior of these mixtures. Supporting Information of values used in the LBC and Peng–Robinson models are provided in Tables 2 and 3. The viscosity data can be reproduced by applying the aforementioned LBC model and using the critical volume data reported in Table 2. In short, with LBC and Peng–Robinson EoS fitted to experimental data, Peng–Robinson EoS was then used for calculating the thermodynamics and phase behavior of these five mixtures without the shear-rate effect (i.e., $f_i(\dot{\gamma}=0)$), and then Eqs. 24 and 30 were used to account for the shear-rate effect on the critical properties and the spinodal curve. These calculations were carried out by solving the conditions of criticality, first and second derivatives of fugacity with respect to mole number, for multicomponent mixtures using the numerical algorithm described by Stockfleth and Dohrn.[28]

Table 4 depicts the results of solving the criticality conditions for the fluids F1–F5, showing not only the effect of shear rate on the liquid–vapor critical point but also the compositional effect. This last one is evident because at the same shear rate value, the differences in critical properties are directly related to the compositional differences among these five reservoir fluids. As it is shown, critical temperature,*Tc*, always increases for the two gases but diminishes very slightly for the three oils. Values of *Tc* for gaseous mixtures are more sensitive to shear rate than for the oils. These oils only show an appreciable reduction in *Tc* for very high shear rates (e.g., 5000 s^{-1}). On the contrary, the values of *Pc* always tend to decrease for both gases and oil mixtures; meaning that a mixing process is always favored if a shear rate is applied. But this point is better analyzed by the spinodal curve behavior; where a particular analysis for the spinodal curves and their variation with shear rate is required. For instance, Figures 1 and 2 depict the spinodal curves against shear rate for F1 (gas) and F4 (oil), respectively. Both figures show that the two-phase region is reduced with increasing shear rate. In other words, in both cases, the shear rate produced a mixing effect, even though the *Tc* showed different trends, upward for F1 and downward for F4. Other important fact is that for F1, the spinodal curve exhibits initially (i.e., $\dot{\gamma}=0$) an ascendant branch at low temperatures, related directly with a liquid–liquid transition in the bubble point curve of the respective bimodal curve; but this liquid–liquid transition is changed to an ordinary liquid–

Table 2. Critical Constants and Other Properties Required by the Peng–Robinson EoS for Modeling the Phase Behavior of the Five Real Petroleum Reservoir Fluids (F1–F5) Used in this Work, with and without Shear Rate Effect

Component	MW [−]	TC [K]	PC [bar]	VC [m^3/kg-mol]	ω [−]	S [−]	Ωa [−]	Ωb [−]
CO_2	44.01	304.2222	73.8639	0.0935	0.2250	−0.0865	0.45724	0.0778
C1N2	16.13	189.9833	45.9195	0.1144	0.0129	−0.0701	0.45724	0.0778
C2	30.07	305.4389	48.7876	0.1651	0.0986	−0.0702	0.45724	0.0778
C3–C4	51.87	390.0278	40.4094	0.2467	0.2099	−0.0450	0.45724	0.0778
C5–C6	79.72	482.3944	32.9451	0.3292	0.2395	0.0203	0.45724	0.0778
C7–C10	126.68	605.6333	27.2509	0.4957	0.3290	0.0526	0.45724	0.0778
C11–C14	195.39	610.8722	20.9219	0.6557	0.4370	0.0778	0.45724	0.0778
C15–C20	214.01	700.6167	15.2518	1.0109	0.5516	0.0849	0.45724	0.0778
C21–C29	347.05	836.8278	12.2638	1.4461	0.7880	0.1004	0.45724	0.0778
C30+	510.21	935.2333	10.7019	1.6923	1.1496	0.1341	0.45724	0.0778

The Critical Volumes (VC) areRequired by the Lorenz–Bray–Clark Viscosity Model.

Table 3. Binary Interaction Coefficients Matrix Required by the Peng–Robinson EoS for Modeling the Phase Behavior of the Five Real Petroleum Reservoir Fluids (F1–F5) Used in this Work

Component	CO_2	C1N2	C2	C3–C4	C5–C6	C7–C10	C11–C14	C15–C20	C21–29	C30+
CO_2	0									
C1N2	0.09938	0								
C2	0.13	0.00081	0							
C3–C4	0.1309	0.00336	0.00089	0						
C5–C6	0.12076	0.00748	0.00342	0	0					
C7–C10	0.11887	0.09142	0.0124	0.00504	0.0008	0				
C11–C14	0.11859	0.09304	0.01822	0.00905	0.00216	0.00036	0			
C15–C20	0.11859	0.10283	0.03291	0.01827	0.00625	0.00267	0.00003	0		
C21–C29	0.11847	0.10549	0.04897	0.02799	0.01083	0.00607	0.00011	0	0	
C30+	0.11849	0.10954	0.05488	0.03601	0.01343	0.00809	0.0002	0.00001	0	0

Table 4. Critical Properties (*Tc* and *Pc*) vs. Shear Rate Predicted for the Five Real Petroleum Reservoir Fluids (F1–F5) Used in this Work

	Reservoir Fluids									
	F1 (gas)		F2 (gas)		F3 (oil)		F4 (oil)		F5 (oil)	
	TC (K)	PC (bar)	TC (K)	PC (bar)	TC (K)	PC (bar)	TC (K)	PC (bar)	TC (K)	PC (bar)
Shear Rate (s−1)										
0	354.46	388.70	396.36	402.13	662.02	234.37	732.32	172.53	796.48	117.60
250	356.32	388.03	397.26	401.34	662.03	234.28	732.30	172.49	796.44	117.58
500	388.08	383.40	399.67	399.19	662.08	234.01	732.25	172.38	796.33	117.55
1000	389.58	377.84	407.43	391.91	662.27	232.95	732.02	171.94	795.91	117.39
1500	391.56	371.46	416.29	382.62	662.52	231.26	731.62	171.24	795.20	117.14
2000	394.48	363.34	424.76	372.68	662.79	229.05	731.06	170.25	794.21	116.79
5000					661.49	209.59	723.29	160.14	782.43	112.53

vapor transition when an sufficiently high shear rate was applied. On the contrary, F4 always shows an ordinary liquid–vapor transition. Finally, for both fluids, the spinodal region at temperatures lesser than the respective critical temperature (i.e., bubble point curve on the bimodal curve) is very much sensitive to shear rate than the part at higher temperatures (i.e., dew point curve on the bimodal curve); meaning that a shear rate affects mainly the lower temperature region because these mixtures have higher viscosities. The aforementioned results for these real multicomponent mixtures are in concordance with those reported by Roming and Hanley[19] for Lennard–Jones binary mixtures,[12] where a suppression of the gas–liquid and liquid–liquid transitions, and therefore an enlargement of the homogeneous region (mixing effect), was reported. Our results also agree with the findings of Antonov et al.[29] based on SALS and turbidity measurements, who showed that for a ternary gelatin–dextran–water biopolymeric system the shear rate can induce a transition from a two-phase state to a homogeneous state (mixing effect), and close to the critical point the effect of shear on the phase equilibrium is not significant. Both findings by Antonov et al.[29] are also represented in this work by checking in Figures 1 and 2, where the sensitivity of the spinodal curve to a shear rate applied is stronger far away from the respective critical points than close to them, particularly in the region where the liquid to gas transition (bubble points curve) occurs. Obviously, a strong effect on spinodal curve is directly linked to a similar effect on the phase equilibrium (vapor–liquid region), and the vapor–liquid region suffers shrinkage (mixing effect) as a result of the shrinkage of the spinodal curve; where the spinodal curve represents the diffusional stability limit and encloses the unstable region of the multicomponent mixture.[30] It is very importance to clarify that the composition of the fluid itself has a strong effect on the spinodal curves and it is easily observed by comparing the respective shapes and magnitudes of the spinodal curves in Figure 1 [fluid 2 (gas), 64.18 mol% of C1N2] and Figure 2 [fluid 4 (oil), 45.03 mol% of C1N2]. For instance, the outmost envelope given by the spinodal curves in Figure 1 covers a PT range very different when compared with that of Figure 2 and is given by the spinodal curve without a shear rate applied on the fluid; meaning that this is obviously a pure compositional effect. Naturally, a shear rate applied can change the shape and magnitude of the spinodal curve as is evidenced in Figure 1, where, for example, a shear rate equal to 2000 s^{-1} caused the disappearance of the ascending

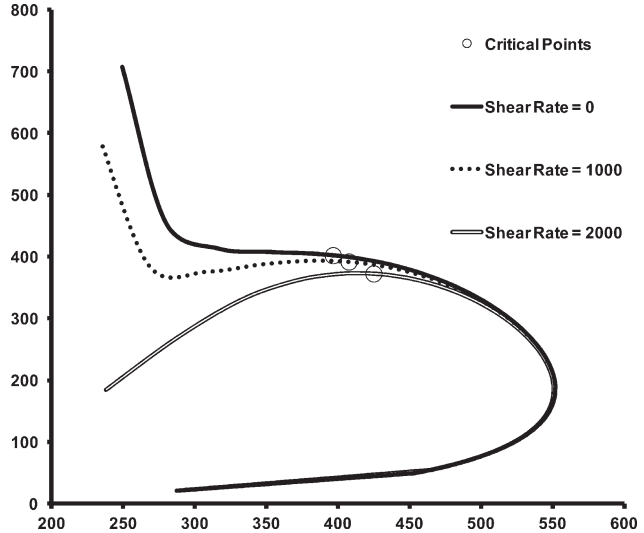

Figure 1. Spinodal curves vs. shear rate for the mixture F2 (gas).

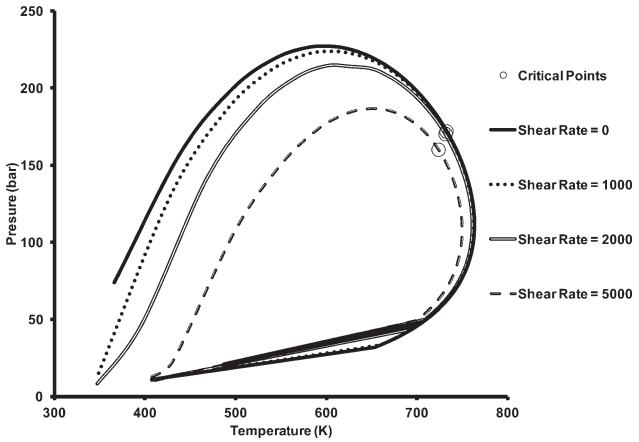

Figure 2. Spinodal curves vs. shear rate for the mixture F4 (oil).

branch, which is typical of liquid–liquid transitions, producing a change from a liquid–liquid equilibrium to a liquid–vapor equilibrium.

Conclusions

A thermodynamic framework for modeling the phase equilibrium of pure fluids and fluid mixtures under the influence of an applied shear rate (shear stress) was derived. This approach is based on the assumption that the viscosity for mixtures can be represented by a power law. Two real gaseous mixtures and three real oil mixtures from South America's petroleum reservoirs were modeled, and it was found that the effect of shear rate on the critical temperature, critical pressure, and spinodal curve of these mixtures depends on the composition of the mixtures. The critical temperature exhibited an upward or downward shift with the shear rate depending on the composition of the mixture, whereas the critical pressure always showed a downward tendency. For the five fluids modeled here, their respective spinodal curves always resulted in a reduction in the unstable region with shear rate, meaning that the shear rate caused a mixing effect. These last results agree with those based on molecular simulations of Lennard–Jones binary model mixtures and experimental measurements based on SALS and turbidity measurements.

Notation

A = Helmholtz free energy
f = fugacity
$\tilde{f}$ = shear-induced chemical fugacity
F = fluid mixtures
G = Gibbs free energy
H = enthalpy
l = work coordinate
L = work coefficient
m = mixture property
N = Mol
NC = number of components
P = pressure
R = universal gas constant
S = entropy
T = temperature
U = internal energy
V = total volume
v = molar volume
W = work.

Greek letters

ξ = exponent in Eq. 16 (viscosity power law)
τ = shear stress
$\dot{\gamma}$ = shear rate (s^{-1})
$\bar{\kappa}$ = intercept in Eq. 16 (viscosity power law)
η = Newtonian viscosity
μ = chemical potential
$\tilde{\mu}$ = shear-induced chemical potential.

Subscripts

i,j = component indexes.

Superscripts

0 = pure component.

Literature Cited

1. Guggenheim EA. Thermodynamics: An Advanced Treatment for Chemists and Physicists, 5th ed. Amsterdam: North Holland Publishing, 1967.
2. Callen HB. Thermodynamics, 2nd ed. New York: John Wiley & Sons, Inc., 1960.
3. Modell M, Reid RC. Thermodynamics and Its Applications, 2nd ed. Englewood Cliffs, New Jersey: Prentice Hall, Inc., 1983.
4. Zimmels Y. Thermodynamics in the presence of electromagnetic fields. *Phys Rev E*. 1995;52:1452–1464.
5. Silberberg A, Kuhn W. Miscibility of liquids influenced by rate of shear. *Nature*. 1952;170:450–451.
6. Jou D, Casas-Vázquez J, Criado-Sancho M. Thermodynamics of Fluids Under Flow. Berlin: Springer, 2000.
7. Onuki A. Phase Transition Dynamics. Cambridge: Cambridge University Press, 2002.
8. Hindawi A, Higgins JS, Weiss RA. Flow-induced mixing and demixing in polymer blends. *Polymer*. 1992;33:2522–2529.
9. Chopra D, Vlassopoulos D. Shear-induced mixing and demixing in poly(styrene-co-maleic anhydride)/poly(methyl methacrylate) blends. *J Rheol*. 1998;42:1227–1947.
10. Rangel-Nafaile C, Metzner A B, Wissbrun KF. Analysis of stress induced phase separation in polymer solutions. *Macromolecules*. 1984;17:1187–1195.
11. de Moel K, Flikkema I, Szleifer G, ten Brinke G. Flow-induced phase separation in polymer solutions. *Europhys Lett*. 1998;42:407–412.
12. Hanley HJM, Evans DJ. A thermodynamics for a system under shear. *J Chem Phys*. 1982;76:3225–3232.
13. Ver Strate G, Philippoff W. Phase separation in flow polymer solutions. *J Polym Sci Polym Lett Ed*. 1974;12:267–275.
14. Wolf BA. Thermodynamic theory of flowing polymer solutions and its application to phase separation, *Macromolecules*. 1984;17:615–618.
15. Marrucci G. Dynamic of entanglements: a nonlinear model consistent with the Cox-Merz rule. *J NonNewtonian Fluid Mech*. 1996;62:279–289.
16. Helfand E, Fredrickson GH. Large fluctuations in polymer solutions under shear. *Phys Rev Lett*. 1989;62:2468–2471.
17. Onuki A. Phase transitions of fluids in shear flow. *J Phys Condens Matter*. 1997;9:6119–6157.
18. Casas-Vázquez J, Criado-Sancho M, Jou D. Dynamical and thermodynamical approaches to phase separation in polymer solutions under flow. *Europhys Lett*. 1993;23:469–474.
19. Roming KD Jr., Hanley HJM. Shear-induced phase changes in mixtures. *Int J Thermophys*. 1986;7:877–885.
20. Mazzanti G, Guthrie SE, Siriota EB. Orientation and phase transitions of fat crystals. *Cryst Growth Des*. 2003;3:721–725.
21. Mehrotra A, Bhat NV. Modeling the effect of shear stress on deposition from "Waxy" mixtures under laminar flow with heat transfer. *Energy Fuels*. 2007;21:1277–1286.
22. Jou D, Casas-Vázquez J, Lebon G. Extended Irreversible Thermodynamics, 4th ed. New York: Springer, 2010.
23. Frenkel D, Smit B. Understanding Molecular Simulation: From Algorithms to Applications, 2th ed. San Diego: Academic Press, 2002.
24. Haase R. Thermodynamics of Irreversible Processes. Massachusetts: Addison Wesley Publishing Company, Inc., 1969.
25. Alberty RA. Use of legendre transforms in chemical thermodynamics. *Pure Appl Chem*. 2001;73:1349–1380.
26. Lohrenz J, Bray BG, Clark CR. Calculating viscosities of reservoir fluids from their compositions. *J Pet Technol*. 1964;16:1171–1176.
27. Peng D-Y, Robinson DB. A new two constant equation. *Ind Eng Chem Fundam*. 1976;15:59–64.

28. Stockfleth R, Dohrn R. An algorithm for calculating critical points in multicomponent mixtures which can easily be implemented in existing programs to calculate phase equilibria. *Fluid Phase Equilib*. 1998;145:43–52.
29. Antonov YA, Van Puyvelde P, Moldenaers P, Leuven KU. Effect of shear flow on the phase behavior of an aqueous gelatin-dextran emulsion. *Biomacromolecules*. 2004;5:276–283.
30. Heidemann RA, Khalil A. The calculation of critical points. *AIChE J*. 1980;26:769–779.

Appendix A

The thermodynamic framework discussed in this article (Eq. 19 or 22) can be used for modeling the effect of a shear rate ($\dot{\gamma}$) on the phase behavior of fluid mixtures (or pure components), if T, V, n_j, and $\dot{\gamma}$ are the variables of interest. But similar expressions can also be deduced starting from Eq. 12 and using T, P, n_j, and τ as the independent variables.[24]

Then, from Eq. 12[2,24]

$$dG \equiv -SdT - \sum_i l_i dL_i + \sum_{i=1}^{NC} \mu_i dn_i \tag{A1}$$

By introducing the coordinates and coefficients of the works related with volumetric expansion (and compression) and shear stress, respectively

$$l_i = V \text{ and } V\dot{\gamma} \tag{A2}$$

$$L_i = -p \text{ and } \tau \tag{A3}$$

Then, Eq. A1 can be simplified to

$$dG \equiv -SdT + VdP - (\dot{\gamma}V)d\tau + \sum_{i=1}^{NC} \mu_i dn_i \tag{A4}$$

By integration of Eq. A4 at T, P, n constants

$$\int_{G_0}^{G} dG = -\int_{\tau=0}^{\tau} V\dot{\gamma} d\tau \tag{A5}$$

Here, we will assume that $\dot{\gamma} = \frac{\tau^{1/\xi}}{\bar{\kappa}^{1/\xi}}$but

$$\dot{\gamma} = \frac{\tau^{1/\xi}}{\bar{\kappa}^{1/\xi}} \tag{A6}$$

Here, we will assume that $V$is independent of τ, and only depends onT, P, n. Obviously, that is not strictly right but it could be a very good approximation

Then

$$\int_{G_0}^{G} dG = -V\int_{\tau=0}^{\tau} \frac{\tau^{1/\xi}}{\bar{\kappa}^{1/\xi}} d\tau \tag{A7}$$

or

$$G = G_0 - \frac{V}{\bar{\kappa}^{1/\xi}} \frac{\tau^{(1/\xi+1)}}{(1/\xi+1)} \tag{A8}$$

The derivation of A8 with respect to n_i, keeping $T, P, \tau, n_{j\neq i}$ as constants, produces

$$\left(\frac{\partial G}{\partial n_i}\right)_{T,P,\tau,n_{j\neq i}} = \left(\frac{\partial G_0}{\partial n_i}\right)_{T,P,n_{j\neq i}} + \frac{1}{(1/\xi+1)\bar{\kappa}^{1/\xi}} \left[\frac{n_t v}{\xi\bar{\kappa}}\left(\frac{\partial \bar{\kappa}}{\partial n_i}\right)_{T,P,\tau,n_j\neq i} - \bar{v}_i\right]\tau^{(1/\xi+1)} \tag{A9}$$

Finally

$$\bar{\mu}_i(\tau) = \mu_i(\tau=0) + \frac{1}{(1/\xi+1)\bar{\kappa}^{1/\xi}} \left[\frac{n_t v}{\xi\bar{\kappa}}\left(\frac{\partial \bar{\kappa}}{\partial n_i}\right)_{T,P,\tau,n_j\neq i} - \bar{v}_i\right]\tau^{(1/\xi+1)} \tag{A10}$$

where $V = n_t v$; $\bar{v}_i = \left(\frac{\partial V}{\partial n_i}\right)_{T,P,\tau,n_{j\neq i}}$ have been used.

In terms of fugacities

$$\tilde{f}_i(\tau) = f_i(\tau=0)\exp\left\{\frac{1}{(1/\xi+1)\bar{\kappa}^{1/\xi}RT}\left[\frac{n_t v}{\xi\bar{\kappa}}\left(\frac{\partial \bar{\kappa}}{\partial n_i}\right)_{T,P,\tau,n_j\neq i} - \bar{v}_i\right]\tau^{(1/\xi+1)}\right\} \tag{A11}$$

For a pure component

$$\bar{\mu}_i^0(\tau) = \mu_i^0(\tau=0) - \frac{v_i^0}{(1/\xi+1)\bar{\kappa}^{1/\xi}}\tau^{(1/\xi+1)} \tag{A12}$$

$$\tilde{f}_i^0(\tau) = f_i^0(\tau=0)\exp\left\{-\frac{v_i^0}{(1/\xi+1)\bar{\kappa}^{1/\xi}RT}\tau^{(1/\xi+1)}\right\} \tag{A13}$$

For a Newtonian mixture, $\xi = 1$ and $\bar{\kappa} = \eta$; then

$$\bar{\mu}_i(\tau) = \mu_i(\tau=0) + \frac{1}{2\eta}\left[\frac{n_t v}{\eta}\left(\frac{\partial \eta}{\partial n_i}\right)_{T,P,\tau,n_j\neq i} - \bar{v}_i\right]\tau^2 \tag{A14}$$

$$\tilde{f}_i(\tau) = f_i(\tau=0)\exp\left\{\frac{1}{2\eta RT}\left[\frac{n_t v}{\eta}\left(\frac{\partial \eta}{\partial n_i}\right)_{T,P,\tau,n_j\neq i} - \bar{v}_i\right]\tau^2\right\} \tag{A15}$$

For a pure Newtonian component

$$\bar{\mu}_i(\tau) = \mu_i(\tau=0) - \frac{v_i^0}{2\eta}\tau^2 \tag{A16}$$

$$\tilde{f}_i(\tau) = f_i(\tau=0)\exp\left\{-\frac{v_i^0}{2\eta RT}\tau^2\right\} \tag{A17}$$

Manuscript received Apr. 19, 2012, and revision received Mar. 10, 2013.